



Original Article

Investigations of Some Chlorocresol Hydrazones Against Tyrosinase Enzyme by Molecular Docking Method: In Silico Study

Necla Kulabas^{ID}, Fahrettin Bugra Kilic^{ID}, Sevil Senkardes^{ID}

Marmara University, Faculty of Pharmacy, Department of Pharmaceutical Chemistry, Istanbul, Türkiye

✉ Corresponding Author: Necla Kulabas (E-mail: necla.kulabas@marmara.edu.tr)

Received: 2025.01.13; Revised: 2025.02.06; Accepted: 2025.02.15

Abstract

Introduction: Tyrosinase, found in various organisms, including plants and mammals, and is responsible for pigmentation as well as the undesirable browning of fruits and vegetables, is a multi-copper enzyme involved in the synthesis of melanin in human. As it is known, melanin provides protection against harmful ultraviolet radiation, which can lead to serious conditions like skin cancers. However, excessive melanin accumulation could result in hyperpigmented spots, creating aesthetic concerns. Tyrosinase inhibitors could potentially lead to the development of novel skin-whitening agents, anti-browning compounds for food preservation, and also for insect control substances. Recently, a wide spectrum of numerous moderate to potent tyrosinase inhibitors have been identified and reported.

Methods: In this study, by using the AutodockVina Virtual Screening Tool, some hydrazide-hydrazone compounds starting from p-chlorocresol were screened for interactions and binding mode of the tyrosinase active site. The enzyme-ligand interactions were analyzed using Biovia Discovery Studio software. Moreover, drug-likeness potential of the compounds was examined by using SwissADME online web tool.

Results: The results showed that compound S5, which did not violate the Lipinski and Veber rules and had a binding energy of -7.9 kcal/mol, could be a potential inhibitor of the tyrosinase enzyme.

Conclusion: Identifying the interactions between the tested ligands and the tyrosinase enzyme will contribute to the development of new hydrazide-hydrazone derivatives aiming the inhibition of tyrosinase.

Keywords: p-chlorocresol, docking, druglikeness, hydrazone, tyrosinase

1. Introduction

Melanin is a pigment produced by specialized cells in the deepest layer of the epidermis and is crucial for safeguarding the skin against the damaging

effects of ultraviolet (UV) radiation (1,2). It also contributes to the color of our skin, eyes, and hair, influencing our overall appearance. While melanin primarily serves a protective role against UV rays, an excess proliferation in certain areas of the skin

can result in hyperpigmentation, which can pose aesthetic concerns (3).

Hyperpigmentation, a common skin condition, resulting from the excessive production or accumulation of melanin, the pigment responsible for skin color (4). This overproduction occurs during the process of melanogenesis, where the tyrosinase (TYR) enzyme catalyzes the oxidation of L-tyrosine to L-dopa, and subsequently to dopaquinone, the precursor of melanin. While melanin provides natural protection against UV radiation, its overproduction can lead to skin disorders like melasma and dark spots (5-7). As a result, TYR inhibitors have gained significant attention not only in the cosmetic but also food industries. In cosmetics, they are used to lighten skin and reduce the appearance of hyperpigmentation, whereas in the food industry, they can prevent browning in fruits and vegetables.

Although several TYR inhibitors are available, some, such as kojic acid and hydroquinone, have raised concerns about safety and long-term efficacy. On the other hand, newer compounds like thiamidol and deoxyarbutin promise safer alternatives (Fig 1). For instance, thiamidol, has demonstrated potent inhibitory effects on TYR, with a clinical trial confirming its efficacy in improving skin tone after topical application. Another compound, deoxyarbutin, has been reported to lighten skin effectively without causing irritation or damage to melanocytes (8).

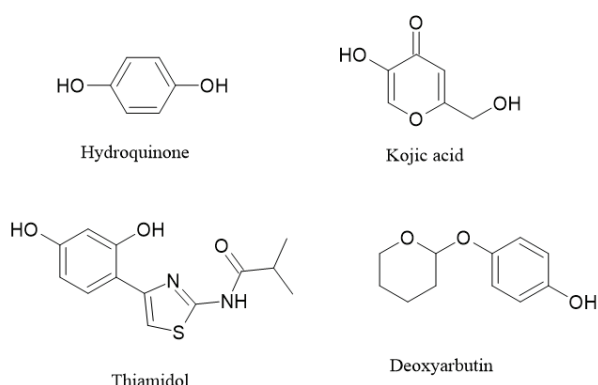


Figure 1. Chemical structures of some tyrosinase inhibitors

Hydrazones are organic compounds characterized by the $-\text{CH}=\text{N}-\text{NH}_2$ functional group, that are

widely used in chemical synthesis as intermediates for the production of heterocyclic compounds, pharmaceuticals, and coordination complexes (9,10). Biologically, hydrazones exhibit diverse therapeutic effects, including antibacterial, antifungal, antiviral, anticancer, and anti-inflammatory activities (11-13). Their structural flexibility makes them valuable in medicinal chemistry for designing compounds with targeted biological properties.

In the current study, the potential inhibitory activity of 2-(4-chloro-3-methylphenoxy)-*N'*-[(aryl)methylidene]acetohydrazides (**S1-10**), which had been synthesized previously by our research group was investigated *in silico* by using molecular docking simulation method (14). Based on the docking studies, among the ten compounds studied, one (**S5**) appeared to have the highest inhibition on TYR activity.

2. Methods

2.1 Chemistry

As shown in Table 1, 2 - (4-Chloro-3-methylphenoxy)-*N'*-[(aryl)methylidene]acetohydrazides (**S1-10**) were successfully synthesized by using a well-known method and the synthetic protocol and spectral data of the molecules (**S1-10**) were reported previously by our research group (14).

2.2 Molecular modeling study

2.2.1 Protein preparation

The recently reported high-resolution X-ray structure of TYR (2.78 Å) (PDB ID 2Y9X: <https://www.rcsb.org/structure/2Y9X>) (15) was used in this study. After acquiring the protein crystal structure, all water molecules were deleted except those located in the ligand binding site. While co-crystallized ligand tropolone was deleted, Cu^{+2} ions in the active site were kept constant. The protein was saved in .pdb format and subsequently converted to pdbqt format using Autodocktools 1.5.6. (16). Then, the region of co-crystallized ligand were determined as the locations of the grid box (-9.923,

-26.885, -43.059) by using Autodocktools 1.5.6. and Discovery Studio 2021 (Accelrys Software Inc., Discovery Studio Modeling Environment, Release 4.0, San Diego, 2013.).

2.2.2 Preparation of the ligands

Compounds **S1-10** were drawn by using Spartan 4.0, and each molecule's energy was also minimized using Spartan 4.0 (17). The most stable isomer, *E*, was selected in the drawing of the all ligands. The conformations with the lowest energy were saved in .pdb format and then converted to .pdbqt format by using Autodocktools 1.5.6. (18,19).

2.2.3 Molecular docking

The determination of the grid box region (-9.923, -26.885, -43.059) and dimensions (40x40x40 Å) to include tropolone was performed using AutodockTools 1.5.6. and Discovery Studio 2021. Molecular docking was subsequently conducted by using Autodock Vina (19), with each docking process repeated a minimum of three times to ensure result accuracy. The docking scores and conformations of each molecule were then visualized by using Discovery Studio 2021, and the

2.3 Determination of druglikeness profile

The present study focuses on evaluating the drug-likeness of compounds **S1-10** according to Lipinski's 5 rules and Veber's rule. All of these compounds were assessed in terms of molecular weight, LogP, number of hydrogen bond donors/acceptors, topological polar surface area, and the number of rotatable bonds (20). Additionally, these compounds were examined for gastrointestinal (GI) absorption and blood-brain barrier (BBB) permeability. All of these data were obtained from the online web server SwissADME (21).

3. Result and Discussion

The *p*-chlorocresol hydrazones listed in Table 1 and the co-crystallized ligand tropolone were drawn using Spartan. They were then prepared for docking studies by using AutodockTools 1.5.6. In the first step, docking studies were conducted with tropolone using the parameters reported in

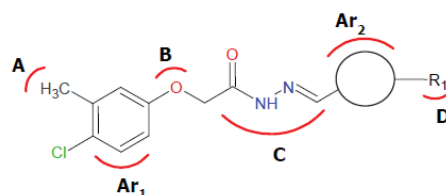


Table 1. Tested compounds **S1-10** and their binding energy against active site of TYR enzyme and their druggability

Compound	Ar ₂	R ₁	Binding Energy (ΔG=kcal/mol)	Lipinski rule n _{viol}	Veber rule n _{viol}
S1	Phenyl	2-Cl,3-OCH ₃	-7.0	0	0
S2	Phenyl	2,5-(OH) ₂	-7.1	0	0
S3	Phenyl	4-OCF ₃	-6.9	0	0
S4	Phenyl	3-OCH ₃ , 4-F	-7.1	0	0
S5	Phenyl	2,6-(CH ₃) ₂	-7.9	0	0
S6	Phenyl	2,6-F ₂	-7.3	0	0
S7	Thiophene	4-C ₆ H ₅	-7.3	0	0
S8	Pyrazole	3-C ₆ H ₅	-7.7	0	0
S9	Phenyl	2-OCF ₃	-6.9	0	0
S10	Phenyl	3-NO ₂ , 4-CH ₃	-7.1	0	0
Tropolone			-5.5		

binding energies of all ligands for each molecule are summarized in Table 1.

the material and method section. In the mentioned validation study, a similarity was observed between

the tropolone placed in the active site with the co-crystallized ligand tropolone, with a RMSD value of 1.029 Å. Subsequently, the binding potentials of compounds **S1-10** to the tyrosinase enzyme were investigated.

When the results of molecular modeling studies were examined, it was determined that the p-chlorocresol ring of compounds **S4**, **S6**, **S7**, **S9**, and **S10** was located in the tropolone binding site. In terms of hydrogen bond interactions, the hydrazone group (C) of molecules **S6** and **S7** forms H-bond interactions with the His244 amino acid at distances of 2.36 Å and 1.88 Å, respectively. Additionally, the hydrazone group (C) of the **S4** molecule interacted with the Val283 amino acid through an H-bond at a distance of 2.46 Å. Hydrogen bond interactions of all compounds with the active site, via substituents (D) on the hydrazone side chain, were identified and

presented in Fig 2. Furthermore, compounds **S4**, **S6**, and **S9**, which contain -F substitution, exhibit halogen interactions with the active site (Fig 2).

Analysis of the hydrophobic interactions between the compounds in Fig 2 and the active site reveals that the p-chlorocresol ring, the starting material, engaged in pi-sigma interactions with the Val283 amino acid. Additionally, compound **S6** exhibited a pi-anion interaction with the Glu322 amino acid, while compound **S10** formed a pi-cation interaction with the His285 amino acid. Compounds **S4** and **S10** displayed pi-pi T-shaped interactions with the active site, whereas compound **S7** demonstrated a pi-pi stacked interaction. The hydrophobic interactions (pi-alkyl and alkyl) of the mentioned compounds with amino acids Leu63, Ala80, Phe192, His259, His263, Phe264, Val283, Pro284, and His285 enhanced their affinity for the active site.

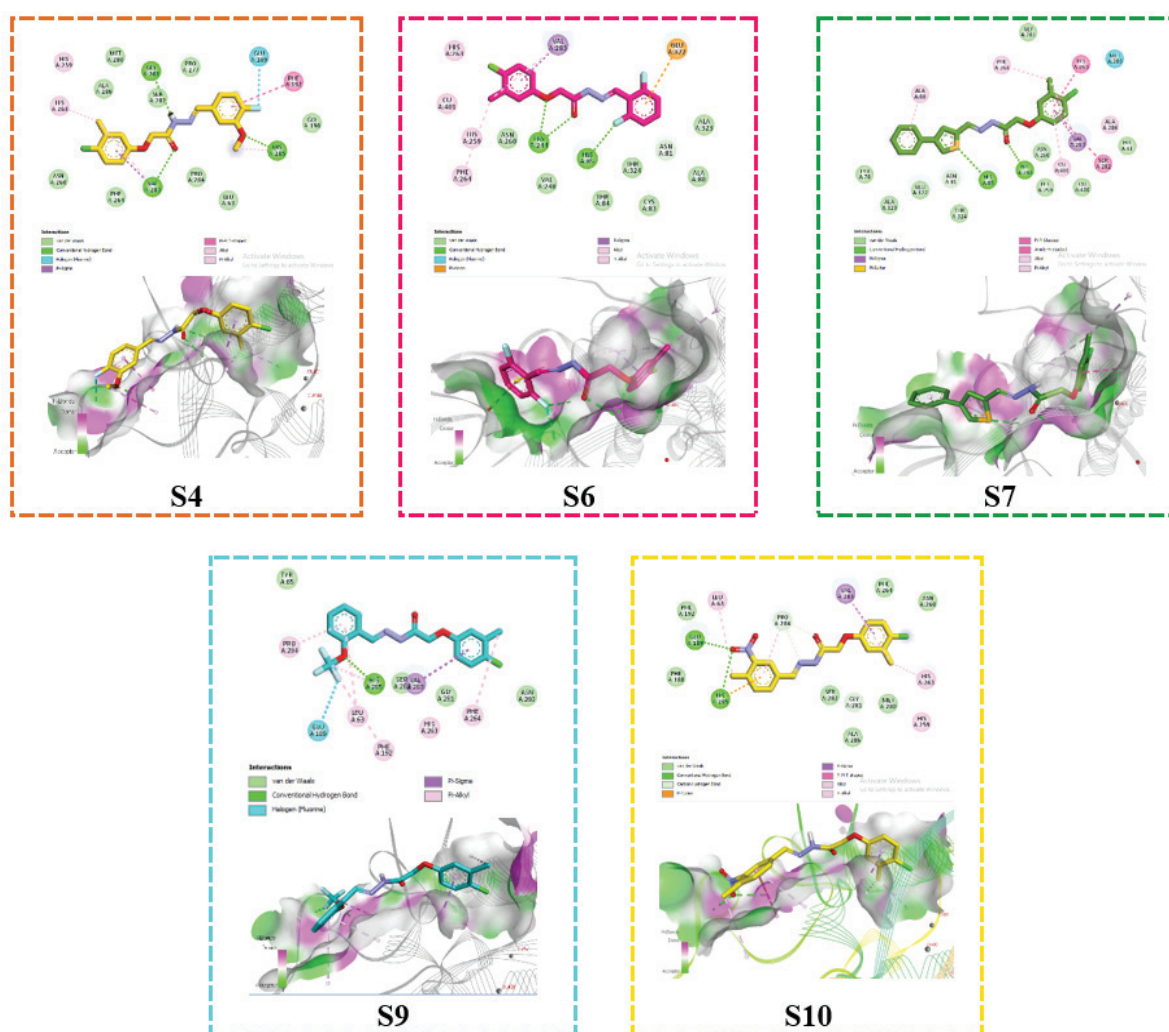


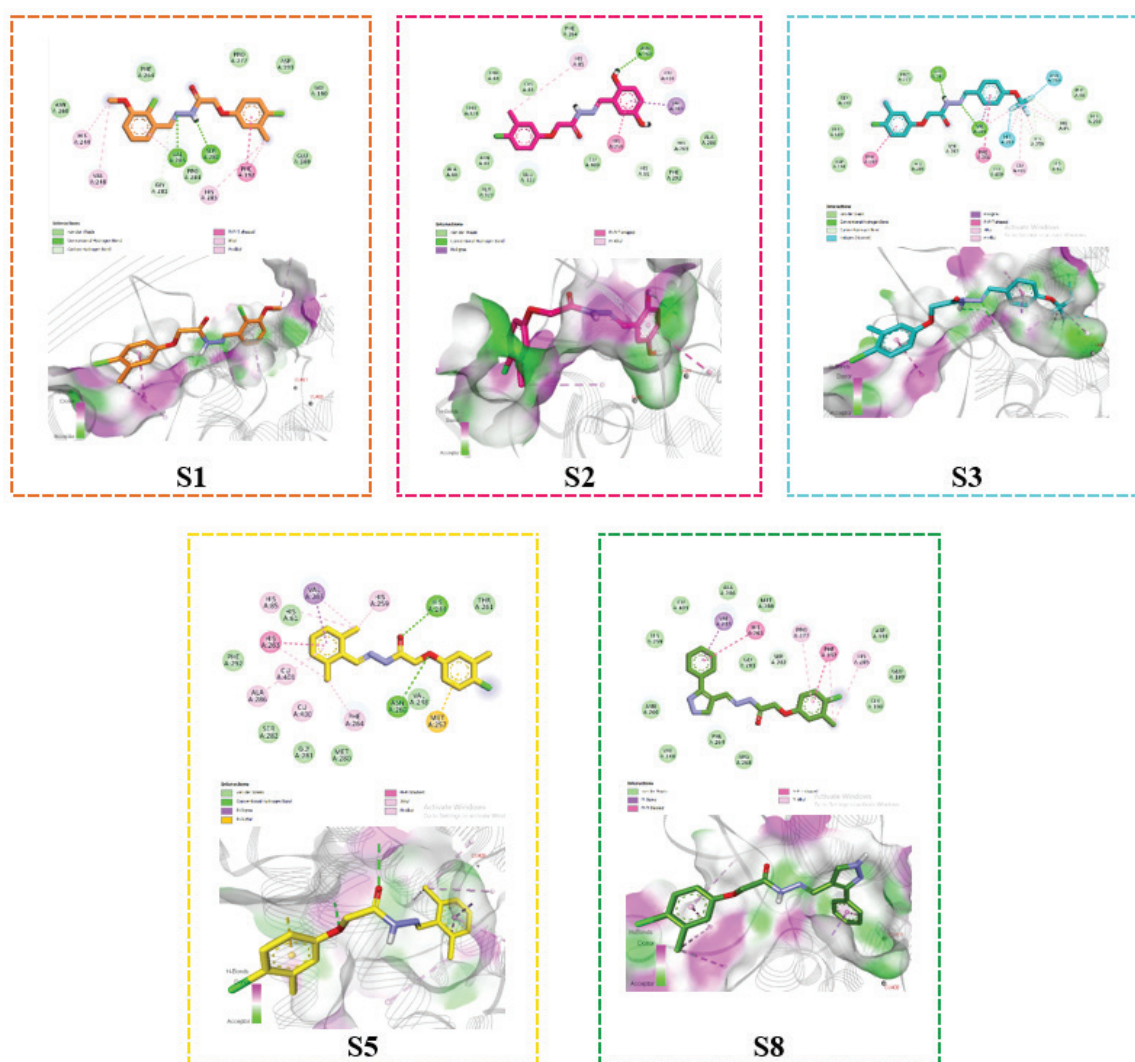
Figure 2. The interactions of compounds **S4**, **S6**, **S7**, **S9**, and **S10** with the active site of the TYR enzyme.

Table 2. Interactions of compound **S5** with the active site of tyrosinase enzyme (**S5** is yellow, tropolone is red).

	Func. Group	Residue	Interaction	Distance (Å)
	B	Asn260	H-bond	2.83
	C	His244	H-bond	2.88
	D	Val283	Alkyl	4.86
	D	His263	Pi-Alkyl	4.44
	D	His85	Pi-Alkyl	4.61
	D	Phe264	Pi-Alkyl	4.76
	D	His259	Pi-Alkyl	4.97
	Ar ₁	Met257	Pi-Sulfur	3.75
	Ar ₂	Val283	Pi-Sigma	3.56
	Ar ₂	His263	Pi-Pi Stacked	4.00
	Ar ₂	Ala286	Pi-Alkyl	4.99

When the results of molecular modeling studies for compounds **S1**, **S2**, **S3**, **S5**, and **S8** were examined, it has been determined that the phenyl ring in the hydrazone side chain is positioned in the tropolone

binding site. In terms of hydrogen bond interactions, the hydrazone group of the **S1** molecule formed H-bond interactions with the Val283 and Ser282 amino acids at distances of 2.10 Å and 2.36 Å,

**Figure 3.** The interactions of compounds **S1**, **S2**, **S3**, **S5**, and **S8** with the active site of the TYR enzyme.

respectively. Similarly, the **S2** molecule formed H-bond interactions with the Asn260 amino acid at a distance of 2.52 Å through the phenol group in its hydrazone side chain, while no H-bond interaction with the active site was detected for the **S8** molecule. The hydrazone group of the **S3** molecule formed H-bond interactions with Val283 and Gly281 amino acids at distances of 2.70 Å and 2.74 Å, respectively. Additionally, the $-OCF_3$ group in the side chain of the hydrazone group interacted via halogen bonds with the His259, Asn260, and His263 amino acids (Fig 3).

Examining the hydrophobic interactions of the compounds depicted in Fig 3 with the active site has revealed that the p-chlorocresol ring, the starting material, engages in pi-pi T-shaped interactions

well as between its ether (*B*) chain and the Asn260 amino acid at a distance of 2.83 Å. Lastly, it is thought that pi-sulfur interactions with the Met257 amino acid contributed to its binding energy.

The BOILED-Egg model is a tool used to predict the passive gastrointestinal (GI) absorption and brain access of small molecules, which is useful for drug discovery and development. It provides a simple graphical estimation of passive intestinal absorption and brain penetration as a function of WLOGP and TPSA. When the plotted molecule falls inside the white ellipse, good intestinal absorption is expected, while falling inside the yellow ellipse indicates a high probability of crossing the blood-brain barrier (BBB). Molecules located in the gray area are predicted to neither be absorbed by the GI tract nor

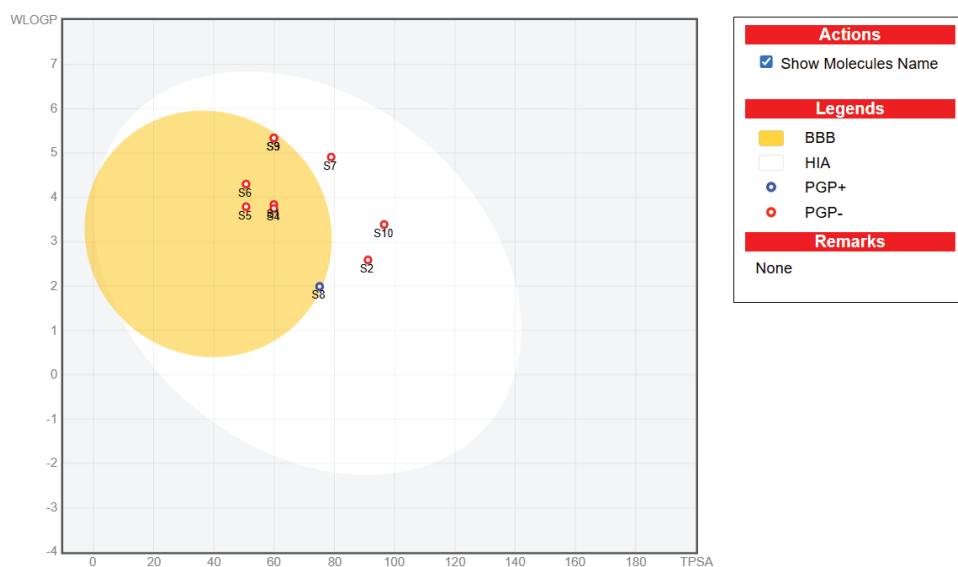


Figure 4. Graphical distribution of compounds **S1-S10** using the boiled egg predictive model.

with the amino acids Phe192, Phe264, and His259, as well as pi-sigma interactions with Val283. Additionally, hydrophobic interactions (pi-alkyl and alkyl) between these compounds and amino acids His85, Phe192, His244, Val248, His263, Phe264, Pro277, Val283, and His285 further has enhanced their affinity to the active site.

Among the compounds **S1-S10**, the compound predicted to have the highest in silico TYR inhibition has been **S5**, with a binding energy of -7.9 kcal/mol (Table 2). For compound **S5**, an H-bond interaction was identified between its hydrazone C=O group and the His244 amino acid at a distance of 2.88 Å, as

cross the BBB (21). Based on this information, it is predicted that compounds, except for **S2**, **S7**, and **S10**, can cross the BBB and have high GI absorption. Additionally, none of the compounds, except **S8**, are Pgp substrates (Fig 4).

4. Conclusion

In conclusion, the docking study conducted in this study clarifies the molecular interactions between the compounds **S1-S10**, previously synthesized by our research group, and the *Agaricus Bisporus* Mushroom Tyrosinase enzyme, sheds light on the TYR enzyme inhibition potential of the compounds.

The hydrazone group in the compounds was observed to interact with the enzyme binding site via hydrogen bonding, reinforced by hydrophobic interactions, and demonstrated a higher binding energy than the co-crystallized ligand, tropolane. When examining the drug-likeness potential of the compounds, it was determined that they do not violate either Lipinski's or Veber's rules, and their predicted GI absorption and BBB permeability were presented using the boiled-egg model. Among the tested compounds, **S5** ($\Delta G = -7.9$ kcal/mol) showed the highest affinity, displaying a binding profile characterized by hydrogen bonds, hydrophobic interactions, and electrostatic contacts. The identification of hydrogen bond interactions between the hydrazone group of the tested ligands and TYR enzyme will contribute to the development of new hydrazide-hydrazone derivatives targeting enzyme inhibition.

Conflicts of interest: The authors declare no conflicts of interest related to this work.

Ethics approval: Not applicable

References

- Maddodi N, Jayanthi A, Setaluri V. Shining light on skin pigmentation: the darker and the brighter side of effects of UV radiation. *Photochem Photobiol.* 2012;88(5):1075-1082. <https://doi.org/10.1111/j.1751-1097.2012.01138.x>
- Brenner M, Hearing VJ. The protective role of melanin against UV damage in human skin. *Photochem Photobiol.* 2008;84(3):539-549. <https://doi.org/10.1111/j.1751-1097.2007.00226.x>
- Thawabteh AM, Jibreen A, Karaman D, Thawabteh A, Karaman R. Skin Pigmentation Types, Causes and Treatment- A Review. *Molecules.* 2023;28(12). <https://doi.org/10.3390/molecules28124839>
- Karakaya G, Türe A, Ercan A, Öncül S, Aytemir MD. Synthesis, computational molecular docking analysis and effectiveness on tyrosinase inhibition of kojic acid derivatives. *Bioorg Chem.* 2019;88:102950. <https://doi.org/10.1016/j.bioorg.2019.102950>
- Ebanks JP, Wickett RR, Boissy RE. Mechanisms regulating skin pigmentation: the rise and fall of complexion coloration. *Int J Mol Sci.* 2009;10(9):4066-4087. <https://doi.org/10.3390/ijms10094066>
- Varghese PK, Abu-Asab M, Dimitriadis EK, Dolinska MB, Morcos GP, Sergeev Y V. Tyrosinase Nanoparticles: Understanding the Melanogenesis Pathway by Isolating the Products of Tyrosinase Enzymatic Reaction. *Int J Mol Sci.* 2021;22(2). <https://doi.org/10.3390/ijms22020734>
- Guo L, Li W, Gu Z, Wang L, Guo L, Ma S, Li C, Sun J, Han B, Chang J. Recent Advances and Progress on Melanin: From Source to Application. *Int J Mol Sci.* 2023;24(5). <https://doi.org/10.3390/ijms24054360>
- Zolghadri S, Beygi M, Mohammad TF, Alijanianzadeh M, Pillaiyar T, Garcia-Molina P, Garcia-Canovas F, Munoz-Munoz J, Saboury AA. Targeting tyrosinase in hyperpigmentation: Current status, limitations and future promises. *Biochem Pharmacol.* 2023;212:115574. <https://doi.org/10.1016/j.bcp.2023.115574>
- Şenkardeş S, Kucukguzel SG. Recent Progress on Synthesis and Anticancer Activity of 4-Thiazolidinone. *Mini-Rev. Org. Chem.* 2016;13(5):377-388. <https://doi.org/10.2174/1570193X13666160826154159>
- Süzcü P, Şenkardeş S, Gürboğa M, Özakpınar ÖB, Küçükgül G. Synthesis and biological evaluation of new 4-thiazolidinone derivatives of flurbiprofen. *Org Commun.* 2023;16(1):11-23. <https://doi.org/10.25135/acg.oc.144.2212.2653>
- Ali R, Marella A, Alam T, Naz R. Review Of Biological Activities Of Hydrazones. *Indones J Pharm.* 2012;23(4):193-202.
- Padmini K, Preethi PJ, Divya M, Rohini P, Lohita M, Swetha K, Kaladar P. A Review on Biological Importance of Hydrazones. *Int J Pharma Res Rev IJPRR.* 2013;2(8):43-58. <https://doi.org/10.4103/0975-7406.129170>
- Rollas S, Küçükgül ŞG. Biological activities of hydrazone derivatives. *Molecules.* 2007;12(8):1910-39. <https://doi.org/10.3390/12081910>
- Şenkardeş S, Erdoğan Ö, Çevik Ö, Küçükgül G. Synthesis and biological evaluation of novel aryloxyacetic acid hydrazide derivatives as anticancer agents. *Synth Commun.* 2021;51(17):2634-2643.

<https://doi.org/10.1080/00397911.2021.1945105>

15. Ismaya WT, Rozeboom HJ, Weijn A, Mes JJ, Fusetti F, Wichers HJ, Dijkstra BW. Crystal Structure of Agaricus bisporus Mushroom Tyrosinase: Identity of the Tetramer Subunits and Interaction with Tropolone. *Biochemistry*. 2011;50(24):5477-5486. <https://doi.org/10.1021/bi200395t>
16. Morris GM, Huey R, Lindstrom W, Sanner MF, Belew RK, Goodsell DS, Olson AJ. AutoDock4 and AutoDockTools4: Automated docking with selective receptor flexibility. *J Comput Chem*. 2009;30(16):2785-2791. <https://doi.org/10.1002/jcc.21256>
17. Stewart JJP. Optimization of parameters for semiempirical methods V: Modification of NDDO approximations and application to 70 elements. *J Mol Model*. 2007;13(12):1173-1213. <https://doi.org/10.1007/s00894-007-0233-4>
18. Hamdan M, Kulabaş N, Küçükgülzel İ. In silico Evaluation of H1-Antihistamine as Potential Inhibitors of SARS-CoV-2 RNA-dependent RNA Polymerase : Repurposing Study of COVID-19 Therapy. 2024;21(6):566-576. <https://doi.org/10.4274/tjps.galenos.2024.49768>
19. Allouche AR. Software News and Updates Gabedit-A Graphical User Interface for Computational Chemistry Softwares. *J Comput Chem*. 2012;32(2):174-182. <https://doi.org/10.1002/jcc.21600>
20. Kulabaş N. In silico investigation of novel 5-benzylidene-2-(arylsulfonylhydrazono)thiazolidine-4-ones as potential inhibitors of mPGES-1 and COX-2. *J Res Pharm*. 2023;27(5) (27(5)):2124-2134. <https://doi.org/10.29228/jrp.491>
21. Daina A, Michielin O, Zoete V. SwissADME: A free web tool to evaluate pharmacokinetics, drug-likeness and medicinal chemistry friendliness of small molecules. *Sci Rep*. 2017;7:1-13. <https://doi.org/10.1038/srep42717>

Cite this article: Kulabas N, Kilic BF, Senkardes S. Investigations of Some Chlorocresol Hydrazones Against Tyrosinase Enzyme by Molecular Docking Method: In Silico Study. *Pharmedicine J*. 2025;2(1);16-23. DOI: 10.62482/pmj.23